TMV induces RNA decay pathways to modulate gene silencing and disease symptoms

Gabriela Conti[1,2], Diego Zavallo[1], Andrea L. Venturuzzi[1,2], Maria C. Rodriguez[1], Martin Crespi[3] and Sebastian Asurmendi[1,2,*]
[1]*Instituto de Biotecnología, CICVyA, INTA, Hurlingham, Argentina,*
[2]*CONICET, Hurlingham, Argentina, and*
[3]*Institute of Plant Sciences Paris-Saclay, IPS2, CNRS, INRA, University Paris-Sud, Orsay, France*

SUMMARY

RNA decay pathways comprise a combination of RNA degradation mechanisms that are implicated in gene expression, development and defense responses in eukaryotes. These mechanisms are known as the RNA Quality Control or RQC pathways. In plants, another important RNA degradation mechanism is the post-transcriptional gene silencing (PTGS) mediated by small RNAs (siRNAs). Notably, the RQC pathway antagonizes PTGS by preventing the entry of dysfunctional mRNAs into the silencing pathway to avoid global degradation of mRNA by siRNAs. Viral transcripts must evade RNA degrading mechanisms, thus viruses encode PTGS suppressor proteins to counteract viral RNA silencing. Here, we demonstrate that tobacco plants infected with TMV and transgenic lines expressing TMV MP and CP (coat protein) proteins (which are not linked to the suppression of silencing) display increased transcriptional levels of RNA decay genes. These plants also showed accumulation of cytoplasmic RNA granules with altered structure, increased rates of RNA decay for transgenes and defective transgene PTGS amplification. Furthermore, knockdown of RRP41 or RRP43 RNA exosome components led to lower levels of TMV accumulation with milder symptoms after infection, several developmental defects and miRNA deregulation. Thus, we propose that TMV proteins induce RNA decay pathways (in particular exosome components) to impair antiviral PTGS and this defensive mechanism would constitute an additional counter-defense strategy that lead to disease symptoms.

Keywords: RNA decay, exosome, TMV, PTGS, defense, symptoms.

INTRODUCTION

RNA plant viruses produce significant reprogramming of host gene expression (Whitham *et al.*, 2003, 2006; Va *et al.*, 2008) and the transcriptional changes because of this reprogramming are usually associated with the occurrence of symptoms (Golem and Culver, 2003; Bazzini *et al.*, 2007; Culver and Padmanabhan, 2007; Conti *et al.*, 2012). In plants, the post-transcriptional gene silencing (PTGS), which is mediated by antiviral small RNAs (vsiRNAs), constitute an important mechanism to control viral infections. This versatile defense response is so widespread that has driven most viruses to evolve viral suppressors of RNA silencing (VSRs) to attenuate or inhibit this process (Qu and Morris, 2005; Siddiqui *et al.*, 2008). VSRs hijack or inhibit antiviral PTGS by interfering with different steps of PTGS. However, simultaneously, the endogenous gene silencing mechanisms are altered, thus producing miRNA deregulation. This finding led to the hypothesis that the disease symptoms are originated by the interference of VSRs with host gene expression regulation (Chapman *et al.*, 2004; Bazzini *et al.*, 2007, 2009, 2011; Wieczorek and Obrępalska-Stęplowska, 2014; Zavallo *et al.*, 2015).

RNA decay pathways constitute an integral and very well conserved mechanism to control endogenous gene expression, by eliminating dysfunctional transcripts to control the quality and abundance of mRNAs (Belostotsky and Sieburth, 2009; Chiba and Green, 2009; Schoenberg and Maquat, 2012). RQC pathways involve many types of ribonucleolytic activities, whose regulation varies depending on their mRNA substrates or physiological conditions.

The RQC activities involve deadenylation, 3′ to 5′ exonucleolytic decay, decapping and 5′ to 3′ exonucleolytic decay. The cytoplasmic decay process typically initiates with deadenylation (removal of mRNA 3′ poly A-tail) followed by 5′ to 3′ exonucleolytic degradation (Sarowar

et al., 2007; Liang et al., 2009). The 3′ to 5′ exonucleolytic degradation requires the action of a ubiquitous multiprotein complex, the RNA exosome, which in plants consists of many subunits making up the central or core region (RRP4, RRP40, RRP41, RRP42, RRP43, RRP45 [CER7], RRP46, and CSL4 MTR3). Additional components involved in the activity of this complex include RRP44, RRP6 (L1, L2, L3) and MTR4 (Chekanova et al., 2007; Vanacova and Stefl, 2007; Schmid and Jensen, 2008; Shin et al., 2013). Furthermore, the degradation of RNA in the 5′ to 3′ direction requires a previous decapping step (removal of mRNA 5′-CAP structure) (Iwasaki et al., 2007; Arribas-Layton et al., 2012; Thran et al., 2012). The nuclear XRN2 and XRN3 (in the nucleus) and the cytoplasmic XRN4 (Potuschak et al., 2006; Gy et al., 2007) execute the exonucleolytic 5′ to 3′ degradation.

In plants, RNA decay pathways and PTGS are intertwined and act on associated ribonucleoproteins. Many of the RQC factors (DCP1, DCP2, DCP5, XRN4 and AGO1) are associated with cytoplasmic processing bodies (P-bodies) (Xu and Chua, 2011; Maldonado-Bonilla, 2014), whereas several PTGS enzymes are localized in juxtaposed cytoplasmic granules (siRNA bodies or SGS3/RDR6 siRNA bodies) (Kumakura et al., 2009; Jouannet et al., 2012; Moreno et al., 2013). RQC degrading activities reduce the accumulation of aberrant mRNAs and prevent their entry into the PTGS pathways. This results in a decreased production of siRNAs, which are potentially mobile and capable of silencing-related sequences. More interestingly, certain mRNAs are also substrates for RDR6-mediated PTGS; hence, RQC activities attenuate the generation of siRNA from these mRNAs. RQC and PTGS compete or act antagonistically (Gazzani et al., 2004; Christie et al., 2011; Martinez de Alba et al., 2015; Zhang et al., 2015). Zhang et al. (2015, 2016) have proposed that the most important function of a mRNA decay mechanism is to avert the PTGS directed against endogenous transcripts.

Animal infecting viruses avoid the RNA decay machinery to maintain the stability of viral transcripts (Moon et al., 2012; Moon and Wilusz, 2013; Narayanan and Makino, 2014). For example, vaccinia virus and other poxviruses encode enzymes for both cap synthesis and decapping. These viruses evolved the ability to exploit the RNA decay machinery by promoting the increased turnover of host mRNAs, thus resulting in the removal of competing endogenous mRNAs and shutdown of host protein synthesis (Parrish et al., 2007; Liu et al., 2014). Additionally, several evidences established an interplay between animal virus infections and RNA granules (Lloyd, 2012, 2014; White and Lloyd, 2012). For instance, the disruption of RNA granules is a common strategy used by viruses to reprogram host gene expression in animal systems. However, much less information is known on plant viral infections.

In this work, we studied the effect of individual Tobacco Mosaic Virus (TMV) proteins as well as virus infections on RNA decay mechanisms and consequently on the development of symptoms. We demonstrated that the RNA decay machinery is targeted by TMV infection. Hence, we proposed that plant viruses hijack proper RQC regulation to counteract PTGS and in this way they have evolved a strategy in relation to their animal counterparts.

RESULTS

Transcripts involved in RNA decay and PTGS, P-bodies and si-bodies are altered in TMV-infected plants and MP × CP^{T42W} transgenic tobacco plants

To analyze the influence of TMV in RQC and PTGS, we measured the accumulation of a selection of genes related to these pathways in wild type Nicotiana tabacum 'Xanthi' infected with TMV. The infected plants (TMV) were compared to non-infected and non-transgenic controls (NI) at two stages of infection, early and late (6 and 18 dpi respectively). Figure S1 displays the viral levels at the analyzed stages. In parallel, transgenic lines expressing TMV proteins were also used to analyze the same genes. The transgenic tobacco lines expressing individual TMV proteins were the following: (a) CP^{T42W}, (b) MP, and (c) MP×CP^{T42W}. The CP^{T42W} transgenic line carries a mutated version of the TMV CP with a point mutation on Tyr^{42} changed to Trp (Bendahmane et al., 1997; Asurmendi et al., 2004). The MP transgenic line expresses the TMV movement protein and finally MP×CP^{T42W} is a double transgenic line produced from a cross between the CP^{T42W} and MP lines. Although the transgenic expression of CP^{T42W} shows no altered phenotype in tobacco, when compared with CP transgenic plants, it induces a resistance response stronger than the one induced by the native CP (Bendahmane et al., 1997). It is worth mentioning that neither the individual viral proteins nor the double expression of CP^{T42W} and MP show PTGS suppressor activity (Bazzini et al., 2007).

We detected significant increases in mRNA accumulation of RNA exosome complex components RRP41, RRP43 and RRP6 in the MP × CP^{T42W} transgenic line and of components RRP41, RRP43 in late stages of TMV infection (Figure 1), (Log-2 expression ratios and P-values are detailed in Table S1). The DCP1 transcript, which is involved in decapping, showed significantly higher levels of expression in TMV late stage of infection and in the MP × CP^{T42W} transgenic line. Genes involved in PTGS (RDR1, AGO1, DCL1, RDR6 and SGS3) were strongly induced in late stages of TMV infections, as expected, but remained unchanged in the MP × CP^{T42W} line (with the exception of SGS3, which was up-regulated). RDR1, a PTGS amplification component linked to antiviral defense mediated by salicylic acid, showed remarkable reduced levels in the CP^{T42W} and MP×CP^{T42W} lines; which suggests an effect of

CP on the defense pathways mediated by salicylic acid (Conti *et al.*, 2012; Rodriguez *et al.*, 2014). By contrast, XRN3 and XRN4 were significantly induced exclusively at early stages, thus showing an expected differential response along the time course of infection. The expression pattern of RQC genes in MP $\times$ CP^{T42W} is similar to the one observed at late stages of TMV infection, when CP reached maximum accumulation and, consequently, showed their predominant effects. However, at early stages, the prevailing replicase protein could be the main factor controlling the response.

P-bodies and si-bodies are altered in TMV-infected plants and MP $\times$ CP^{T42W} transgenic line

Subsequently, we examined the subcellular location of RNA granules (P-bodies and si-bodies) in tobacco leaf tissues by transiently expressing marker genes and translational fusions to fluorescent reporters (GFP). Interestingly, both TMV-infected plants and the MP $\times$ CP^{T42W} transgenic line showed larger P-bodies (marked by DCP1::GFP fusion) and siRNA bodies (marked by SGS3::GFP fusion) (Jouannet *et al.*, 2012; Moreno *et al.*, 2013). RRP41::GFP fusion, which potentially marks RNA exosome core complexes, showed enhanced accumulation in those plants (Figure 2a). Statistical analyses were performed with five to seven images for

each line and more than 15 measurements for each picture, by measuring granule size (pixels) in the case of DCP1 and SGS3 fusion and regions of interest intensity (ROIs) in the case of RRP41 fusion (Figure 2b). The data clearly correlated with the previous idea that MP $\times$ CP^{T42W} line and TMV infection increased size of P-bodies, si-bodies and RRP41 ROIs intensity. We also tested co-localization of TMV-CP and P-bodies when DCP1::RFP fusion was co-expressed with 35S:TMV-CP::GFP constructs (Figure 2c). A significant co-localization rate was evident, given by Pearson co-localization coefficient which averages selected ROIs (Figure 2d). These results suggest that the RQC machinery is spatially associated to viral replication complexes.

Overall, we hypothesize that the activation of the RNA decay pathways and the alteration of its different components in RNA granules could be part of a plant defense response induced to degrade and reduce the accumulation of viral RNAs. Alternatively, and more interestingly, this activation could mean a viral counter-defense strategy evolved to prevent PTGS of viral RNA, which may also contribute to the reprogramming of plant gene expression observed in viral infections.

Induced mGFP decay progression is altered in MP $\times$ CP^{T42W} plants

To study the impact of viral proteins (MP $\times$ CP^{T42W}) and TMV infections on RNA decay progression, we performed two experimental set ups to measure the amount of aberrant RNA degradation in each tobacco line. As a first strategy, we designed a construct expressing a GFP transcript carrying a point mutation that generates a premature termination codon (GFP–PTC) and consequently a long 3′ UTR. These GFP–PTC transcripts, when transiently expressed by agroinfiltration in tobacco leaves, are rapidly detected and degraded by non-sense mediated decay pathway (NMD) (Kertész *et al.*, 2006) where the RNA exosome complex plays a pivotal role (Figure 3a).

As a second strategy, we measured the decay of GFP transcript 3′ fragments induced by miRNA cleavage. In this case, we expressed a GFP construct together with an artificial miRNA construct directed to GFP (miR–GFP) to induce cleavage and subsequent degradation (Figure 3b). The constructs were transiently expressed in the MP $\times$ CP^{T42W} transgenic line, TMV-infected plants and NI controls. Absolute RT-qPCR assays were performed to measure accumulation levels of GFP transcripts. The amount of aberrant GFP degradation was calculated by comparing full length native GFP expression (reference) versus GFP–PTC or GFP + miR–GFP at different time points (raw data is shown in Table S3).

These strategies allowed us to compare the differential accumulation of aberrant GFP transcripts in the MP $\times$ CP^{T42W} transgenic line and TMV-infected plants compared to NI controls. For instance, transcript degradation induced by GFP–PTC was higher in the MP $\times$ CP^{T42W}
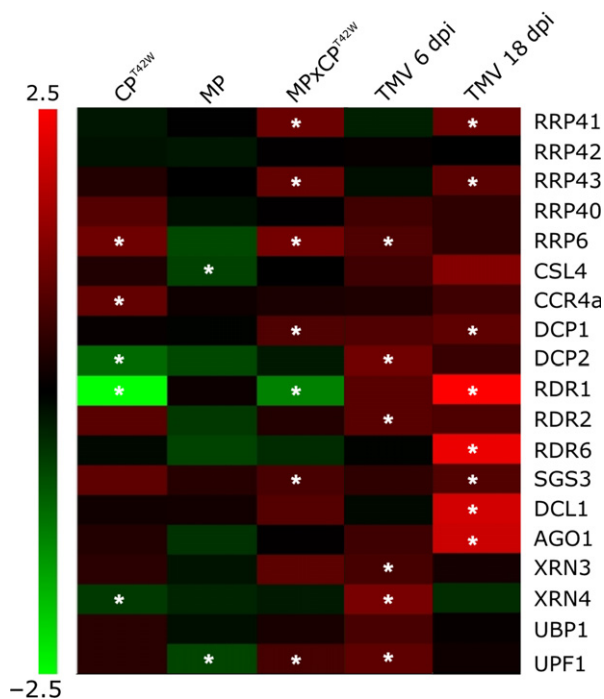
Figure 1. RNA decay and PTGS transcript levels are altered in the MP $\times$ CP^{T42W} and TMV-infected tobaccos.
Heat map illustrating data of RT-qPCR analysis (log-2 ratios) of RNA decay and PTGS pathway transcripts in the tobacco CP^{T42W}, MP and MP$\times$CP^{T42W} transgenic lines and at early and late stages of TMV infection (6 and 18 dpi) compared to NI controls. *Indicates significant differences with *P*-values <0.05.
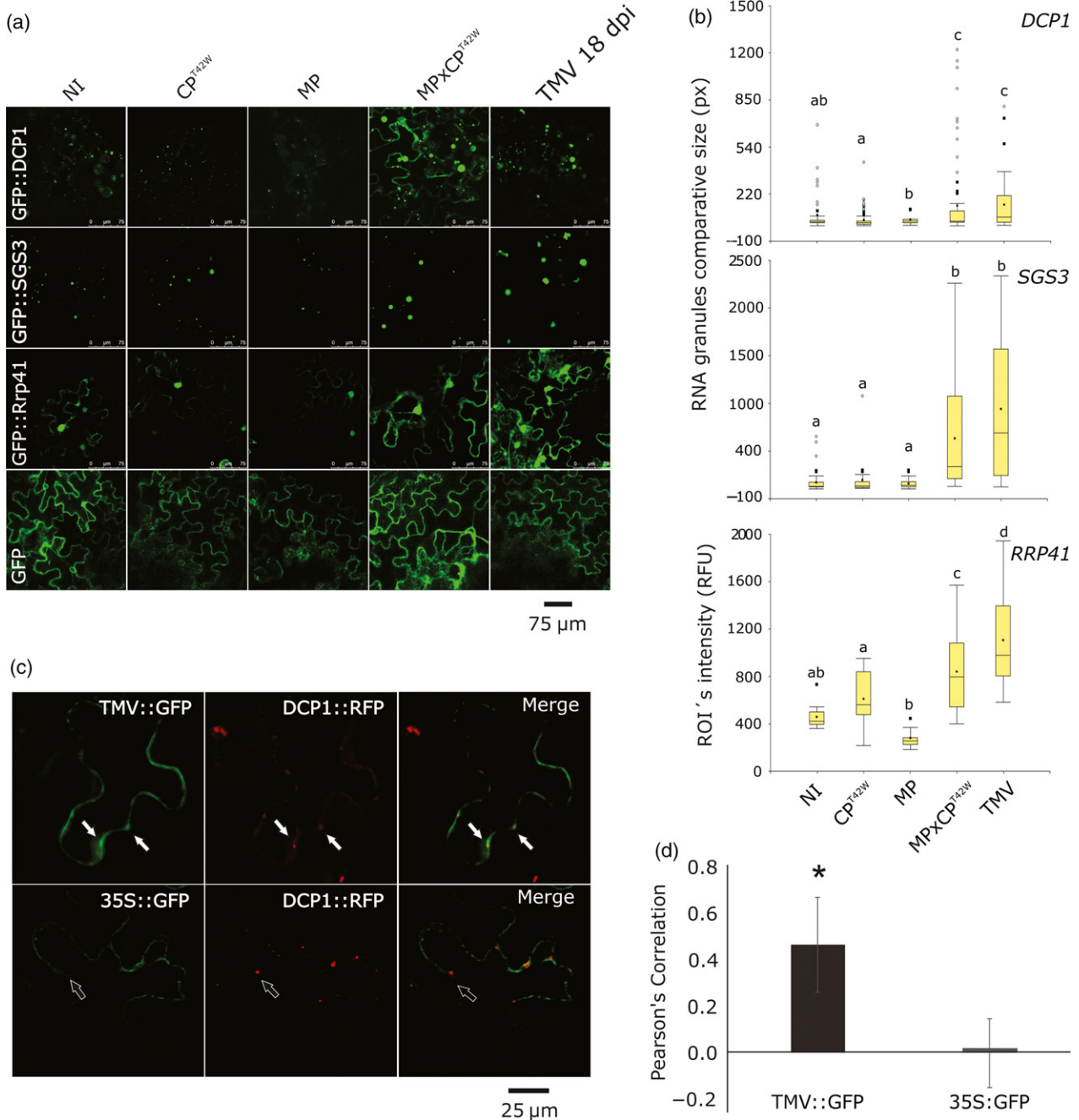
Figure 2. RNA granules (P-bodies and si-bodies) show altered structure in the MP × CP^{T42W} plants and TMV infections and are closely associated with active viral replication sites.

(a) Confocal section images showing subcellular localization of the indicated fluorescent fusion proteins in tobacco leaves of transgenic lines and at different stages of TMV infection compared to NI controls.

(b) The box-plot graphs show comparative statistics of P-bodies and si-bodies size measurements and fluorescence intensity of several regions of interest (ROIs intensity level) in RRP41 expressing cells. The letters 'a' and 'b' are indicative of significant differences with *P*-values <0.05.

(c) Confocal section images of TMV-CP::GFP infected (second column) and GFP expressing *N. benthamiana* leaves (first column) with the co-expression of RFP:: DCP1 and merged images (third column) demonstrating co-localization of P-bodies with TMV replication active sites. The white arrows indicate co-localization, whereas the open arrows indicate foci positive for only one of the two fusion proteins. The scale bars are shown on the images.

(d) The graph shows selected ROIs and Pearson's correlation coefficient of several images indicating significant co-localization. *Indicates significant differences with *P*-values <0.05.
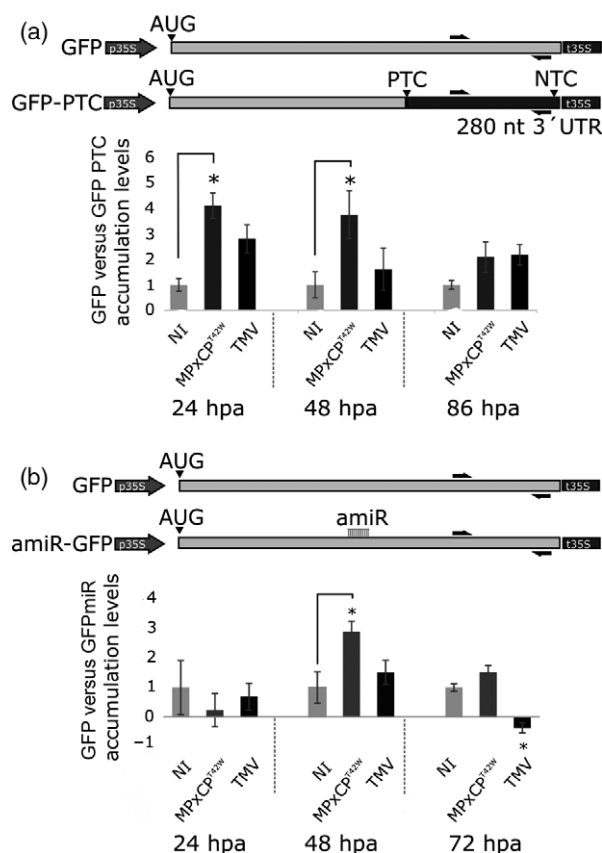
Figure 3. Degradation of aberrant transiently expressed GFP transcript is altered in the MP × CP^T42W plants and in TMV infections when compared to NI controls.
(a) Absolute RT-qPCR data representing the differences between transient accumulation of mGFP (reference) and GFP–PTC constructs (source of aberrant transcripts) at the indicated time points.
(b) Absolute RT-qPCR data representing differences between transient accumulation of mGFP (reference) and GFP + miR–GFP constructs (source of aberrant transcripts) at the indicated time points. For both experiments, the mean differences of transcript levels (log-2 of molecules number ± standard error) of five replicates is shown. *Indicate statistical significant differences with *P*-values <0.05 by ANOVA test.

transgenic line than in NI controls (difference between GFP versus GFP–PTC absolute accumulation levels). This difference was statistically significant at 24 and 48 h post agroinfiltration (hpa). TMV-infected plants showed a similar but attenuated effect (Figure 3a and Table S3). For the second strategy, we analysed an amplicon localized in the 3′ region of the transcript (Figure 3b) to estimate aberrant GFP transcript degradation (difference between absolute GFP and GFP + miR–GFP absolute accumulation levels). At 48 hpa, this degradation was significantly higher in the MP × CP^T42W transgenic line, and showed an attenuated effect in the TMV infection. However, at 72 hpa, TMV infection samples showed lower GFP degradation rates than NI control. As expected, this finding suggests a strong interference of the TMV-126 kDa suppressor of silencing on miR–GFP activity (Figure 3b and Table S3). In summary,

the enhanced accumulation of RNA decay transcripts (Figure 1) in response to MP and CP^T42W co-expression functionally correlated with increased GFP–PTC or 3′ miRNA cleavage products degradation rates. This effect also occurred, although attenuated, in TMV infections. This attenuation could be due to the silencing effect of the viral suppressor that may interfere with decay mechanisms.

Deficient transient GFP silencing (S-PTGS) leads to enhanced transgene expression in MP × CP^T42W line

Co-agroinfiltration of the GFP reporter gene with an inverted repeat of GFP (which results in a double-stranded dsGFP) allow us to analyze the PTGS pathway and also to detect silencing suppressor proteins (Roth *et al.*, 2004). Increments in GFP fluorescence/accumulation levels are indicative of a silencing suppression activity. We then analysed the effect of the individual viral proteins and the simultaneous expression of MP and CP on the development of PTGS. For this purpose, we examined transient GFP expression, silencing and suppression of silencing in the MP, CP^T42W, MP × CP^T42W transgenic lines and in TMV infections (Figure 4). GFP was transiently expressed in each line, and also co-agroinfiltrated with different VSRs (HC-Pro, p19 or p38).

Transient GFP fluorescence was higher in the MP×CP^T42W transgenic line (Figure 4a), thus suggesting that GFP transgene expression is enhanced in these plants. This effect was persistent even after HC-Pro, p19 and p38 co-agroinfiltration in all the transgenic lines and in TMV infections. This result suggests that the mechanism indirectly triggered by MP and CP^T42W co-expression could be operating upstream of siRNA biogenesis. These viral proteins show no intrinsically VSR effect when transiently co-expressed with GFP (Bazzini *et al.*, 2007).

To further explore the mechanisms underlying these effects, we subsequently analysed the accumulation of GFP transcripts and small RNAs derived from GFP (sGFP) in agroinfiltrated tissues by Northern blot assays. GFP mRNA (mGFP) accumulated notably more in MP × CP^T42W than in the NI and non-transgenic controls, in agreement with the results obtained at the protein levels (which were measured by fluorescence) (Figure 4b). On the other hand, the TMV-infected plants exhibited similar levels of mGFP accumulation than NI controls.

Subsequently we co-agroinfiltrated GFP construct with different suppressor of silencing proteins to find out if mGFP over-accumulation was persistent in the MP × CP^T42W line. We also assayed this construct together with either p19 or HC-Pro suppressors (Figure 4c). This indicates that mGFP over-accumulation in the MP × CP^T42W transgenic line is independent of the mode of action of these viral proteins on RNA-induced silencing complex (RISC) activity. We also performed northern blot analysis to detect siRNAs against GFP (sGFP).
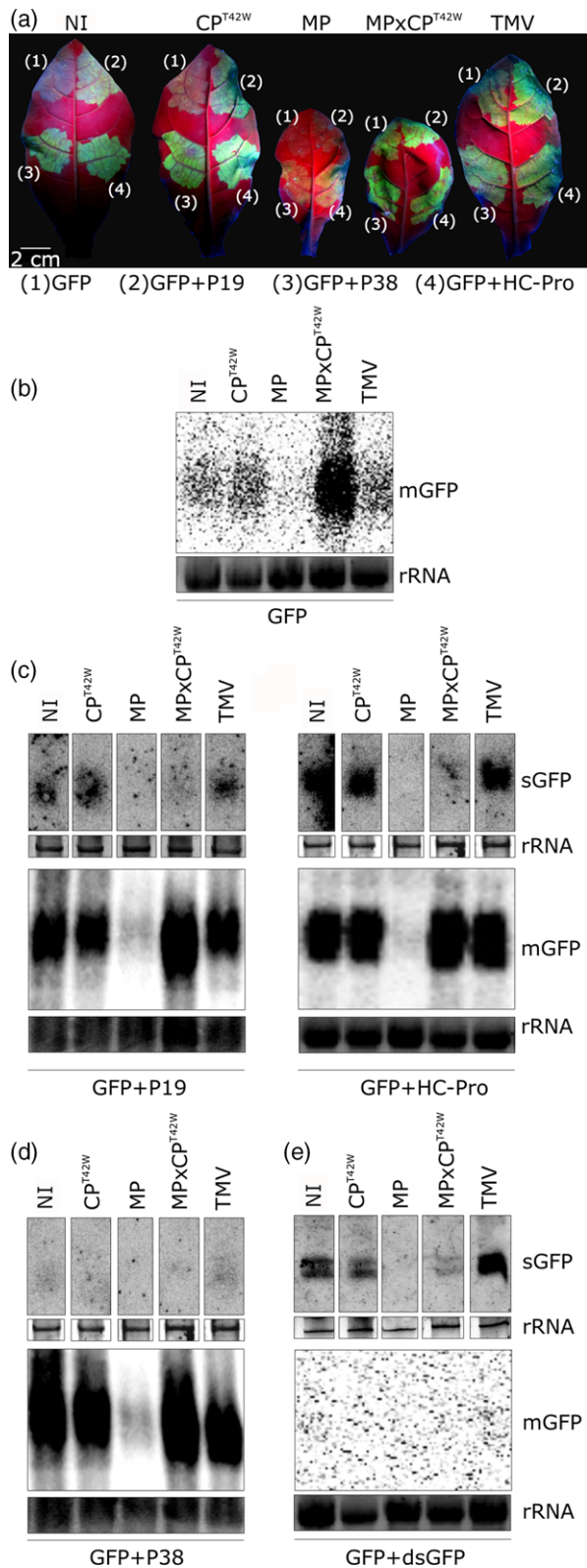
Figure 4. Transient mGFP expression is enhanced in the MP × CP^{T42W} line due to a defective sGFP accumulation.
(a) GFP fluorescence level observed in tobacco leaves after agroinfiltration in the CP^{T42W}, MP, MP × CP^{T42W} transgenic lines and in TMV infections compared with the NI controls. The agroinfiltrated constructs were (1) GFP, (2) GFP + p19, (3) GFP + p38, and (4) GFP + HC-Pro.
(b) Northern blot assay showing high molecular weight GFP transcript (mGFP) of plants agroinfiltrated with GFP construct in all the transgenic lines, TMV infections and NI controls. rRNA was set as reference.
(c) Northern blot assays showing high-molecular-weight (mGFP) and low-molecular-weight (sGFP) for GFP + p19 (left) and GFP + HC-Pro (right) co-agroinfiltrations in all the transgenic lines, TMV infections and NI controls. rRNA was set as reference.
(d) Northern blot assays showing high-molecular-weight (mGFP) and low-molecular-weight (sGFP) for GFP + p38 co-agroinfiltrations in all the transgenic lines, TMV infections and NI controls. rRNA was set as reference.
(e) Northern blot assays showing high-molecular-weight (mGFP) and low-molecular-weight (sGFP) for GFP + dsGFP co-agroinfiltrations in all the transgenic lines, TMV infections and NI controls. rRNA was set as reference.

controls (Figure 4c). Those reductions are in concordance with the increased accumulation of mGFP transcript; which suggests that an endogenous suppressor of silencing effect independent of RISC activities occurs in the MP × CP^{T42W} transgenic line. However, the co-agroinfiltration of GFP with the viral suppressor p38 showed similar amounts of mGFP in MP × CP^{T42W}, TMV-infected plants and NI controls and no sGFPs were detected in any of the lines. This result is in agreement with the proposed mode of action of p38 (inhibition of DCL4 and 2) (Qu *et al.*, 2003) (Figure 4d).

Finally, when GFP was co-agroinfiltrated with a hairpin construct (dsGFP), the levels of GFP transcripts were undetectable (Figure 4e). This finding indicates that PTGS triggered by exogenous dsRNAs is properly active and this was confirmed by the sRNAs accumulation detected in all the lines. Besides this conspicuous sGFP accumulation, which is sufficient to induce PTGS against GFP transcripts, reduced amounts of sGFP were observed in the MP × CP^{T42W} lines. Thus, the mechanism of PTGS amplification may be defective.

The results demonstrate that the co-expression of MP and CP^{T42W} triggers effects that act upstream of RISC complex and Dicer-like (DCLs) activity. Consequently, the reduced S-PTGS observed in the MP × CP^{T42W} plants that leads to an enhanced mGFP accumulation could be produced by a deficient PTGS amplification, which would yield to decreases in secondary siRNAs biogenesis. Therefore, the participation of MP and CP^{T42W} viral proteins in the induction of an endogenous suppression of GFP S-PTGS mechanism could be part of the PTGS antagonistic effect.

VIGS-mediated knock down of RNA exosome components produces developmental defects similar to TMV symptoms and altered miRNAs accumulation in *N. benthamiana*

We then analysed the role of RNA exosome components that were significantly induced in the TMV-infected and the MP × CP^{T42W} plants. For this purpose, we used *Nicotiana*

For both cases, p19 and HC-Pro co-agroinfiltration, a relative reduction of sGFP accumulation level was observed in the MP × CP^{T42W} transgenic line compared to the NI

benthamiana and the *Tobacco Rattle Virus* (TRV)-based virus-induced gene silencing system (VIGS) to knock down gene expression and selected two components of the RNA exosome core structure: RRP41 and RRP43 (Figure 5). Indeed, both components were induced in MP×CP^T42W plants and at late stage of viral infections. *N. benthamiana* plants were agroinfiltrated with pTRV2–*rrp41* and pTRV2–*rrp43* carrying partial *N. tabacum* RRP41 and RRP43 sequences (Table S7); a pTRV–*gfp* construct was used as a control (Figure 5a). The silencing of these genes was confirmed by relative RT-qPCR (Figure 5b).

The reduction of RRP41 and RRP43 expression produced developmental defects such as severe leaf shape distortions and a mosaic-type effect on leaf surface that resemble the typical tobacco TMV symptoms and *N. benthamiana* symptoms under certain conditions (Bubici *et al.*, 2015). The reduction of RRP41 and RRP43 produced changes in the accumulation level of several microRNAs (Figure 5c and Table S4). In fact, the silencing of RRP43 showed more severe effects, with significant decreases of miR164, mir165/166, mir167 and mir172 accumulation and increments of miR398. The RRP41 silencing showed similar outcomes but only for miR167, miR172 and miR398. The side effect of VSRs on miRNAs regulation has been already reported, and as a consequence of their accumulation during viral infections, viral symptoms take place. This link between miRNAs accumulation and viral symptoms has also been well documented. In addition, 3′ to 5′ exoribonucleases regulate the biogenesis and/or turnover of miRNAs (Meng *et al.*, 2011; Lange *et al.*, 2014). Therefore, we suggest that alterations of RRP41 and RRP43 expression also lead to deregulation of miRNA expression and symptom development. This would be similar to those processes occurring during TMV infections.

VIGS-mediated knock down of RNA exosome components produces decreased severity and virus accumulation in TMV infections

To test the impact of the deregulation of exosome components in TMV infections, we inoculated pTRV2–*rrp41* and pTRV2–*rrp43* silenced plants with TMV virions. Interestingly, the typical wilting symptom, which is mediated by stem necrosis, observed in TMV-infected *N. benthamiana* plants was less severe than in pTRV2–*gfp* controls (Figure 6a). Figure 6(b) shows the symptomatology progression by means of quantifying the 'necrosis mediated wilting' symptom in plants that show a reduction of the severity of this phenotype on the two exosome-compromised plants. This reduction of symptoms correlated with diminished virus accumulation (significant for TRV2-*rrp43*) (Figure 6c). These results indicate an active role of RRP41 and RRP43 on TMV symptom development and TMV antiviral defense responses, probably because of the
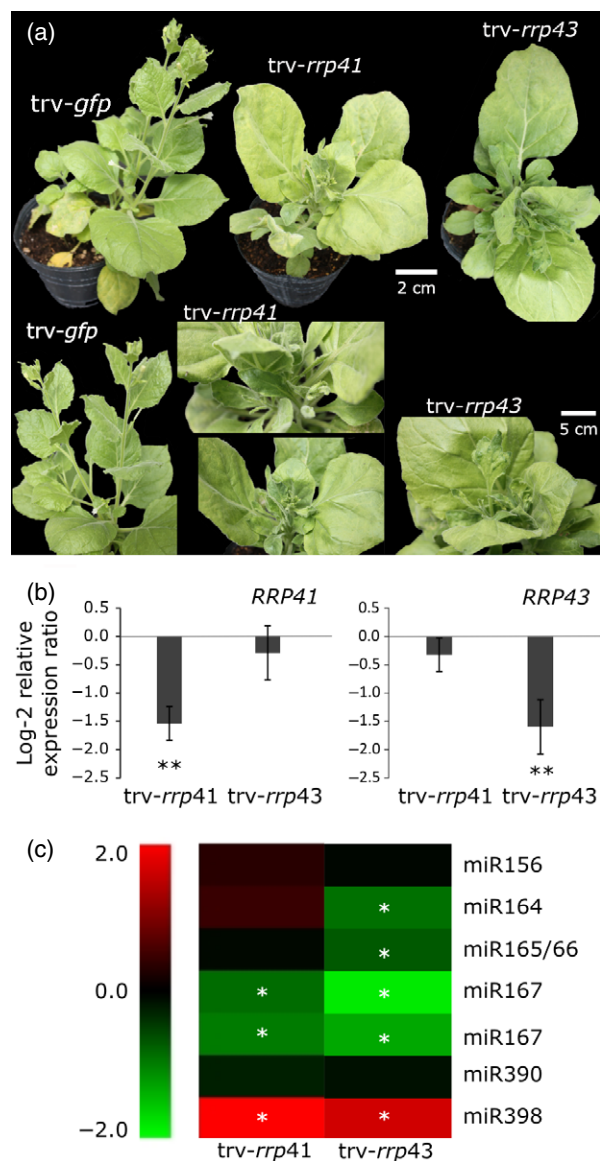
Figure 5. RRP41 and RRP43 silencing mediated by VIGS produces changes in plant development, which resemble TMV symptoms, and alters several miRNAs accumulation levels in *Nicotiana benthamiana*.
(a) Impact on *N. benthamiana* growth and development observed 2 weeks after RRP41 (trv-*rrp*41) and RRP43 (trv-*rrp*43) silencing mediated by VIGS compared to control plants (trv-*gfp*).
(b) Bar graphs showing relative expression ratios by RT-qPCR determination (log-2) of RRP41 an RRP43 transcript levels in trv-*rrp*41 and trv-*rrp*43 compared to trv-*gfp* *N. benthamiana* plants.
(c) Heat map illustrating qRT-PCR relative expression ratios (log-2) of microRNAs accumulation in trv-*rrp*41 and trv-*rrp*43 plants. *Indicates significant differences with *P*-values <0.05.

interaction of the RNA exosome components with PTGS mechanisms.

DISCUSSION

In this study, we assessed the impact of the expression of TMV proteins, which have not yet been linked to the
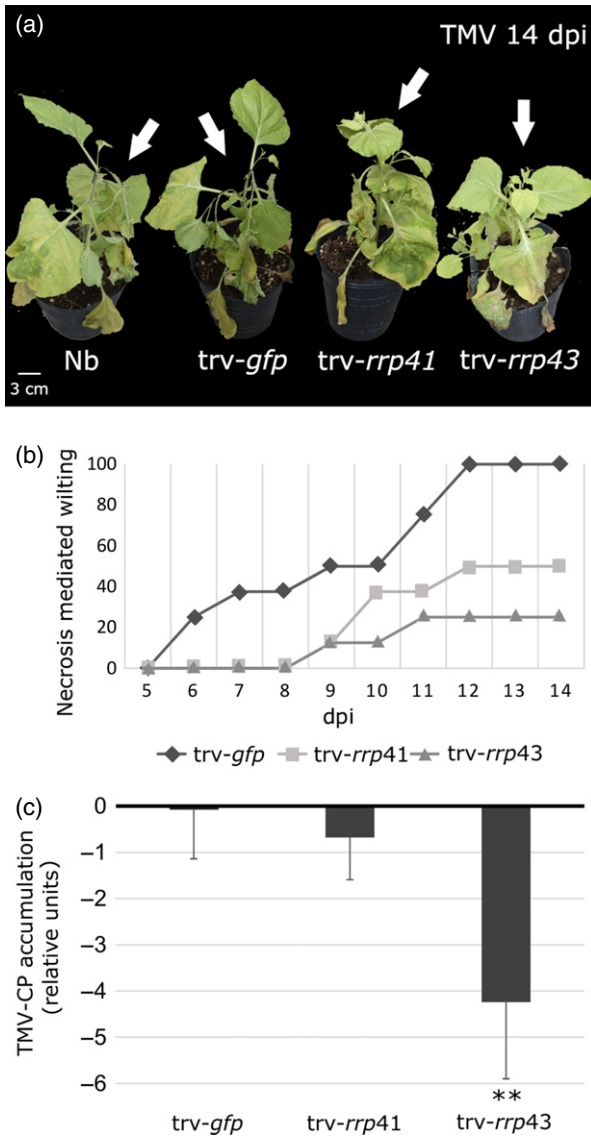
Figure 6. RRP41 and RRP43 silencing mediated by VIGS reduces TMV necrosis-mediated wilting symptoms and diminishes viral titers in *Nicotiana benthamiana* inoculated with TMV.
(a) TMV symptoms displayed by trv-*rrp*41 and trv-*rrp*43 plants are shown with arrows.
(b) The graph shows differential symptom appearance; the percentage of plants with necrosis mediated wilting in trv-*rrp*41, trv-rrp43 and trv-*gfp* controls after the TMV infection was calculated (*n* = 10 plants per treatment).
(c) The TMV infection level was determined as TMV-CP transcript relative accumulation by RT-qPCR. The mean relative transcript levels (log-2) ± standard errors of five replicates are shown. trv-*gfp* plants were used as controls for all experiments. *Indicates significant differences with *P*-values <0.05.

suppression of gene silencing (CP^{T42W} and MP), on RNA decay and PTGS pathways. We studied the individual and combined expression. Our results showed that these TMV proteins, as well as TMV infection, induce several components of the RNA decay machinery, thus resulting in an antagonistic interaction with PTGS pathways. In turn, the

virus may use these proteins to control an endogenous suppression of the silencing pathway to reduce the PTGS-mediated degradation of viral transcripts, which are the targets of PTGS. Thus, here we propose that TMV evolved an additional counter-defense strategy based on the induction of RQC pathways to escape the efficient PTGS pathway.

We demonstrated that several genes involved in RQC and PTGS pathways are up-regulated during TMV infections and by the expression of the individual proteins, even though the effect is different (Figure 1). For instance, only plants expressing TMV CP^{T42W} showed an induced CCR4a expression, whereas the TMV CP^{T42W} and MP × CP^{T42W} double transgenic line induced the expression of the RRP6 nuclear RNA exosome component. However, RRP6 expression was induced only at early stages of TMV infection and this induction was lost at late stages. This finding highlights the complex dynamic regulation along the infection, where several suppressors of gene silencing along with the proteins studied here are expressed. RDR1 expression was down-regulated in the CP^{T42W} line as well as in the MP × CP^{T42W} plants. This effect that is mediated by the TMV-CP was previously reported (Conti *et al.*, 2012; Rodriguez *et al.*, 2014). In those studies, the researchers analysed the negative modulation of SA-mediated antiviral defense, including RDR1 and other SA-responsive transcripts. The effect of the individual expression of MP in tobacco plants did not significantly vary RNA decay and PTGS transcript accumulation. The combined expression of coat proteins (MP × CP^{T42W}), which is more close to the infection dynamics, however, induced several RQC genes. It is important to consider that MP functionality is not easy to assess since MP expressing tobacco plants show an extensively stress response mediated by an enhanced ROS accumulation and activation of SA-dependent mechanisms (Conti *et al.*, 2012). These effects may interfere with transient assays making MP transgenic plants not suitable systems for comparative transient GFP expression which achieve low expression levels (mGFP and siGFP), as we show in Figure 4. The MP × CP^{T42W} transgenic line displayed significantly induced expression of the RNA exosome core components RRP41 and RRP43. This result suggests that both viral proteins could trigger an induction of the RNA decay machinery. This double transgenic plant pattern of expression is similar to the one observed in late TMV infections, when the CP reaches a maximum accumulation. At early stages, the replicase protein may be the main factor driving host responses. It is noteworthy to mention that at early stages of infection, XRN3 and XRN4 are induced, but this induction is lost at late stages. This observation may indicate a differential behaviour for 5′ to 3′ and 3′ to 5′ decay pathways throughout the course of TMV infection.

Neither the expression of the individual proteins (CP^{T42W} or MP) nor the combined expression of both viral proteins

possess canonical PTGS suppression activity; which suggests that the herein observed induction of RNA decay could be another strategy to avert this antiviral defense mechanism. This may be required at later stages of the infection when viral systemic movement is active. The double expression of CP^{T42W} and MP is sufficient to induce several components of the RNA exosome. In line with this idea, some components of the RNA decay machinery, including the bidirectional 3′→5′ and 5′→3′ transcripts, are endogenous suppressors of silencing (reviewed in detail by Liu and Chen, 2016). During late stages of TMV infections, the induction of RNA decay machinery, mainly the RNA exosome components, could be a strategy to reinforce suppression of silencing mediated by the viral suppressor of silencing protein (126-kDa replicase component) (Ding *et al.*, 2004). Tobamovirus PTGS suppressors mostly act by binding sRNA duplexes and inhibiting the assembly of the RISC complex because they cannot affect already loaded vsiRNA (Kurihara *et al.*, 2007). With this in mind, a strategy based on reducing the vsiRNA production could be a very useful complement for the virus counter-defense.

Interestingly, in our study, most genes involved in PTGS machinery were up-regulated in TMV infections, thus indicating that this antiviral defense pathway is strongly induced to counteract the infection. The double induction of PTGS and RNA decay pathways during viral infection supports the interplay between host defenses and viral counter-defense mechanisms. A successful infection could be the result of a balance between host defense responses and virus conter-defense acting together.

Our results demonstrated that increased RNA exosome transcripts levels were accompanied by elevated rates of aberrant RNA degradation in the MP × CP^{T42W} transgenic plants. However, during TMV infection, the increased degradation rates were less evident, either for aberrant GFP decay mediated by a GFP construct carrying a premature termination codon or by an artificial miRNA directed against GFP. Here, we hypothesize that the increased accumulation of viral transcripts in the plant at late stages (18 dpi) could be saturating the RNA decay machinery and therefore the effect on aberrant GFP degradation could be attenuated. Furthermore, the replicase protein, which bears the TMV suppression of silencing activity, could somehow inhibit the increased RNA decay function, as already proposed by Shamandi *et al.* (2015). This group showed that RNASE THREE-LIKE 1 (RTL1) was induced after virus infections. This protein is an RNase III-like enzyme that lacks DCL-specific domain and functions as an endogenous suppressor of silencing. However, some viral proteins that suppress RNA silencing counteracted RTL1 activity. Thus, the GFP increased degradation rates expected to occur on TMV-infected cells could be also counteracted by the silencing suppressor. This process is evident on the MP × CP^{T42W} transgenic line.

This hypothesis led us to further express the idea that the observed level of transcript accumulation in virus infections is the resultant of several mechanisms acting concurrently. The use of transgenic plants expressing a subset of viral proteins could help to unravel the components one by one on the plant host.

Subsequently, we transiently expressed GFP and analysed its silencing. A scarce accumulation of siRNA against GFP in the MP × CP^{T42W} line accompanied by an enhanced transgene expression suggested a deficient S-PTGS. This indicates the presence of an endogenous suppressor of silencing activity. However, the transient expression of GFP was reduced by dsGFP expression, thus suggesting that an external supply of double strand RNA substrates is sufficient to produce silencing. By contrast, the inhibition of DCL4/2 by p38 suppressor of silencing protein produced no sGFPs in any of the tested lines and no changes on the levels of mGFP accumulation.

The described endogenous suppression of silencing seems to be dependent on the RNA decay machinery induction by viral proteins. A similar endogenous suppression due to defective siRNA amplification was evident in certain PTGS mutants: *sde*1 or *rdr*6. These mutants were unable to produce secondary siRNAs and, as expected, they showed enhanced transgene expression (Béclin *et al.*, 2002; Luo and Chen, 2007) and developmental defects (Peragine *et al.*, 2004; Vazquez *et al.*, 2004). In the context of a viral infection, the miss-function of siRNA amplification could be detrimental for plant antiviral defense development (Mourrain *et al.*, 2000; Schwach *et al.*, 2005).

As already reported, PTGS and RNA decay are antagonistically related since they compete for similar RNA substrates (Moreno *et al.*, 2013; Martinez de Alba *et al.*, 2015). In agreement with this, Thran *et al.* (2012) observed enhanced transgene expression and defective secondary siRNA production attributable to DCP2 overexpression in *Arabidopsis thaliana.* Ye *et al.* (2015) also found that AS2, which is an activator of DCP2 decapping activity, functions as an endogenous PTGS suppressor by enhancing GUS expression and reducing siRNA accumulation. They also observed that the geminivirus nuclear shuttle BV1 protein induced AS2 expression, thus rendering infected plants more susceptible to viral infection; which further links RNA decay and viral infection.

Here we showed that the reduction of RRP41 and RRP43 RNA exosome components by means of VIGS in *N. benthamiana* rendered developmental defects and miRNA accumulation changes. Interestingly, *trv-rrp41* and *trv-rrp43* plants inoculated with TMV displayed attenuated development of symptoms and *trv-rrp43* plants also showed a significant reduction of TMV accumulation. We hypothesize that this response could be associated to the miss-function of the RNA exosome, which is more severe after RRP43 reduction, which then will favor the entry of

viral aberrant transcripts into PTGS. Similar results were observed by Ye *et al.* (2015), who found reduced CaLCuV titers in *as2* Arabidopsis mutant plants. Thus, our data suggest that the RRP43 RNA exosome core component could be involved as an endogenous suppressor of gene silencing used by TMV to escape gene silencing.

In summary, in this study we demonstrate that during *TMV* infections, RNA decay pathways are induced by the action of movement and coat protein. This is independent of the action of the replicase protein, a suppressor of PTGS. The induction of RNA decay pathways by the virus may then interfere with PTGS amplification by rapidly degrading 'aberrant' viral transcripts destined to be RNA dependent RNA polymerase substrates. Furthermore, the induction of RNA decay can also be the cause of additional symptom development. Hence, the modulation of RNA decay mediated by aberrant RNA degradation is a novel mechanism involved in the development of plant viral diseases. Hence, plant and animal viruses use endogenous RNA decay mechanisms to reprogram host gene expression during disease process.

EXPERIMENTAL PROCEDURES

Plant materials and plasmid constructs

The transgenic and non-transgenic plants were grown under standard greenhouse conditions or in a growth chamber at 24 to 26°C, under a 16/8 h light/dark cycle. The plasmid constructs and antibiotics are listed in Table S5.

RNA extraction and RT-qPCRs

The experimental conditions used for total RNA extraction, first-strand cDNA synthesis, qPCR reactions and reference gene selection for qPCR analysis were applied following MIQE requirements (Bustin *et al.*, 2009) (Table S6). The normalization method used in the relative RT-qPCR was performed according to the Pfaffl algorithm (Pfaffl, 2001); a Paired permutation test (5000) was performed for the statistical analyses. For all the RT-qPCR experiments, we used a minimum of five up to seven biological replicates and two technical replicates (Figures 1, 5b,c and 6c). The oligonucleotide sequences are listed in Table S2. The sequences were selected based on similarity with *Arabidopsis thaliana* (Table S7). The cut-off for statistically significant differences were set as *, **, and ***, which indicate *P*-values <0.05, 0.01, and 0.005, respectively.

For absolute RT-qPCR analysis of Figure 3, one-way analysis of variance (ANOVA) test with Dunnett or Tukey post-test was performed by using InfoStat software (InfoStat version 2008; Grupo InfoStat. FCA, Universidad Nacional de Córdoba, Argentina). The significance level for all post-tests was set as $\alpha = 0.05$.

Transient GFP expression by *N. tabacum* leaf agroinfiltration

The *Agrobacterium tumefaciens* strain GV3101 carrying the different constructs were used to prepare the agroinfiltration solution (10 mM $MgCl_2$; 10 mM MES and 100 μM acetosyringone), which was set to a final OD_{600} of 1. The samples were assayed 3 days after infiltration.

RNA gel blot analyses

For high-molecular-weight (HMW) RNA gel blots, total RNA was extracted with TRIzol® Reagent (Invitrogen, www.thermofisher.com). separated on a 1.5% agarose electrophoresis gel, stained with Eth. Br (10 mg ml^{-1}) (Promega, www.promega.com). and transferred to a nylon membrane (HybondN⁺, Amersham, www.gelifesciences.com). For low-molecular-weight (LMW) RNA analysis, the extraction was performed by using phenol acid extraction and total RNA was separated on a 17.5% denaturing polyacrylamide electrophoresis gel, stained with EthBr (10 mg ml^{-1}) (Promega) and transferred to a nylon membrane (HybondNX, Amersham). LMW RNA hybridization was at 50°C with SigmaPerfectHyb® buffer (Sigma, www.sigmaaldrich.com). HMW RNA hybridization was at 42°C with ULTRAhyb® Ultrasensitive Hybridization Buffer (Ambion, www.thermofisher.com). Blots were hybridized with DNA probes derived from the cDNA of mGFP4 labeled with ^{32}P-dCTP by a random prime labeling system (Promega).

Confocal microscopy imaging

Agroinfiltrated tobacco leaves were mounted in water and directly imaged on a Leica TCS SP5 Confocal (Leica Microsystems, www.leica-microsystems.com). with 488 nm excitation. GFP and RFP were imaged with 495–530 nm (green channel) and 550–700 nm (red channel) detection windows, respectively. All images were acquired with the same gain settings. For co-localizations, images were taken by sequential acquisition, and subsequently analyzed by calculating the Pearson's correlation coefficient of selected groups of ROIs of five to seven images for each treatment (at least 15 measurements for each image). For this analysis, the co-localization module of the Leica LAS AF software was used. The ROIs consisted of smaller sectors of the images where the fluorescence intensities were quantified. For the statistical analysis of the images in Figure 2(b,c), we employed one-way ANOVA test with the Dunnett post-test by using the InfoStat software (InfoStat version 2008; Grupo InfoStat. FCA, Universidad Nacional de Córdoba, Argentina). The significance level for all post-tests was set as $\alpha = 0.05$.

VIGS

The oligonucleotide sequences used for RRP41 and RRP43 fragment cloning are listed in Table S2. Cloning was performed in *N. tabacum* cDNA. The products were cloned into pCR8/GW/TOPO (Invitrogen) and verified by sequencing; subsequently, they were sub-cloned into pTRV2–GW (Liu *et al.*, 2002) by LR recombination. pTRV2–*rrp41*, pTRV2–*rrp43* and pTRV2–*gfp* (control) were electroporated into the *Agrobacterium sp.* strain GV3101, and selected in LB medium with the proper antibiotics (Table S5). The agroinfiltrations were performed with equivalent pTRV1 and pTRV2 mixtures in *N. benthamiana* plants with four to five leaves, as previously described (Liu *et al.*, 2002). Samples were collected 20 days after infiltration, immediately frozen and stored at −80°C.

TMV infection procedure

For inoculation, a single leaf was dusted with Carborundum and 20 μl of semi-purified TMV virus diluted in 20 mM $NaHPO_4$ (pH 7) was added; then, the surface of the leaf was gently abraded. For viral detection, qRT-PCR experiments were performed as described previously.

Statistical analysis

We employed different statistical analyses for each kind of experiment because of the diversity of the measurements. All of them

are explained in detail in each section of Experimental Procedures.

ACKNOWLEDGEMENTS

SUPPORTING INFORMATION

Additional Supporting Information may be found in the online version of this article.

Figure S1. Accumulation of viral RNAs measured by qRT-PCR.

Table S1. Ratios, Standard Errors and *P*-values used to design Figure 1.

Table S2. Oligonucleotide sequences used.

Table S3. Raw data obtained in absolute qRT-PCR for GFP–PTC and amiR–GFP induced decay experiment of Figure 3.

Table S4. Ratios, Standard Errors y *P*-values used to design Figure 5(c).

Table S5. Plasmid constructs used for agroinfiltration experiments

Table S6. Experimental conditions used for RT-qPCR according to MIQE requirements (Minimum Information for Publication of Quantitative Real-Time PCR Experiments).

Table S7. Identity parameters between *Arabidopsis thaliana* RNA decay genes and *Nicotiana tabacum* homologue sequences.

REFERENCES

Arribas-Layton, M., Wu, D., Lykke-Andersen, J. and Song, H. (2012) Structural and functional control of the eukaryotic mRNA decapping machinery. *Biochim. Biophys. Acta* **1829**, 580–589.

Asurmendi, S., Berg, R.H., Koo, J.C. and Beachy, R.N. (2004) Coat protein regulates formation of replication complexes during tobacco mosaic virus infection. *Proc. Natl Acad. Sci. USA* **101**, 1415–1420.

Bazzini, A.A., Hopp, H.E., Beachy, R.N. and Asurmendi, S. (2007) Infection and coaccumulation of tobacco mosaic virus proteins alter microRNA levels, correlating with symptom and plant development. *Proc. Natl Acad. Sci. USA* **104**, 12157–12162.

Bazzini, A.A., Almasia, N.I., Manacorda, C.A. *et al.* (2009) Virus infection elevates transcriptional activity of miR164a promoter in plants. *BMC Plant Biol.* **9**, 152.

Bazzini, A.A., Manacorda, C.A., Tohge, T., Conti, G., Rodriguez, M.C., Nunes-Nesi, A., Villanueva, S., Fernie, A.R., Carrari, F. and Asurmendi, S. (2011) Metabolic and miRNA Profiling of TMV-infected plants reveals biphasic temporal changes. *PLoS ONE*, **6**, e28466.

Béclin, C., Boutet, S., Waterhouse, P. and Vaucheret, H. (2002) A branched pathway for transgene- induced RNA silencing in plants. *Curr. Biol.* **12**, 684–688.

Belostotsky, D.A. and Sieburth, L.E. (2009) Kill the messenger: mRNA decay and plant development. *Curr. Opin. Plant Biol.* **12**, 96–102.

Bendahmane, M., Fitchen, J.H., Zhang, G. and Beachy, R.N. (1997) Studies of coat protein-mediated resistance to tobacco mosaic tobamovirus: correlation between assembly of mutant coat proteins and resistance. *J. Virol.* **71**, 7942–7950.

Bubici, G., Carluccio, A.V., Cillo, F. and Stavolone, L. (2015) Virus-induced gene silencing of pectin methylesterase protects *Nicotiana benthamiana* from lethal symptoms caused by Tobacco mosaic virus. *Eur. J. Plant Pathol.* **141**, 339–347.

Bustin, S.A., Benes, V., Garson, J.A., Hellemans, J., Huggett, J. and Kubista, M. (2009) The MIQE guidelines: minimum information for publication of quantitative real-time PCR experiments. *Clin. Chem.* **55**, 611–622.

Chapman, E.J., Prokhnevsky, A.I., Gopinath, K., Dolja, V.V. and Carrington, J.C. (2004) Viral RNA silencing suppressors inhibit the microRNA pathway at an intermediate step. *Genes Dev.* **18**, 1179–1186.

Chekanova, J.A., Gregory, B.D., Reverdatto, S.V. *et al.* (2007) Genome-wide high-resolution mapping of exosome substrates reveals hidden features in the Arabidopsis transcriptome. *Cell*, **131**, 1340–1353.

Chiba, Y. and Green, P.J. (2009) mRNA degradation machinery in plants. *J. Plant Biol.* **52**, 114–124.

Christie, M., Brosnan, C.A., Rothnagel, J.A. and Carroll, B.J. (2011) RNA decay and RNA silencing in plants: competition or collaboration? *Front. Plant Sci.* **2**, 99.

Conti, G., Rodriguez, M.C., Manacorda, C.A. and Asurmendi, S. (2012) Transgenic expression of Tobacco mosaic virus capsid and movement proteins modulate plant basal defense and biotic stress responses in *Nicotiana tabacum. Mol. Plant Microbe Interact.* **25**, 1370–1384.

Culver, J.N. and Padmanabhan, M.S. (2007) Virus-induced disease: altering host physiology one interaction at a time. *Annu. Rev. Phytopathol.* **45**, 221–243.

Ding, X.S., Liu, J., Cheng, N.-H., Folimonov, A., Hou, Y.-M., Bao, Y., Katagi, C., Carter, S.A. and Nelson, R.S. (2004) The tobacco mosaic virus 126-kDa protein associated with virus replication and movement suppresses RNA silencing. *Mol. Plant Microbe Interact.* **17**, 583–592.

Gazzani, S., Lawrenson, T., Woodward, C., Headon, D. and Sablowski, R. (2004) A link between mRNA turnover and RNA interference in Arabidopsis. *Science*, **306**, 1046–1048.

Golem, S. and Culver, J.N. (2003) Tobacco mosaic virus induced alterations in the gene expression profile of Arabidopsis thaliana. *Mol. Plant Microbe Interact.* **16**, 681–688.

Gy, I., Gasciolli, V., Lauressergues, D., Morel, J.-B., Gombert, J., Proux, F., Proux, C., Vaucheret, H. and Mallory, A.C. (2007) Arabidopsis FIERY1, XRN2, and XRN3 are endogenous RNA silencing suppressors. *Plant Cell*, **19**, 3451–3461.

Iwasaki, S., Takeda, A., Motose, H. and Watanabe, Y. (2007) Characterization of Arabidopsis decapping proteins AtDCP1 and AtDCP2, which are essential for post-embryonic development. *FEBS Lett.* **581**, 2455–2459.

Jouannet, V., Moreno, A.B., Elmayan, T., Vaucheret, H., Crespi, M.D. and Maizel, A. (2012) Cytoplasmic Arabidopsis AGO7 accumulates in membrane-associated siRNA bodies and is required for ta-siRNA biogenesis. *EMBO J.* **31**, 1704–1713.

Kertész, S., Kerényi, Z., Mérai, Z., Bartos, I., Pálfy, T., Barta, E. and Silhavy, D. (2006) Both introns and long 3′-UTRs operate as cis-acting elements to trigger nonsense-mediated decay in plants. *Nucleic Acids Res.* **34**, 6147–6157.

Kumakura, N., Takeda, A., Fujioka, Y., Motose, H., Takano, R. and Watanabe, Y. (2009) SGS3 and RDR6 interact and colocalize in cytoplasmic SGS3/RDR6-bodies. *FEBS Lett.* **583**, 1261–1266.

Kurihara, Y., Inaba, N., Kutsuna, N., Takeda, A., Tagami, Y. and Watanabe, Y. (2007) Binding of tobamovirus replication protein with small RNA duplexes. *J. Gen. Virol.* **88**, 2347–2352.

Lange, H., Zuber, H., Sement, F.M. *et al.* (2014) The RNA helicases AtMTR4 and HEN2 target specific subsets of nuclear transcripts for degradation by the nuclear exosome in Arabidopsis thaliana. *PLoS Genet.* **10**, e1004564.

Liang, W., Li, C., Liu, F., Jiang, H., Li, S., Sun, J., Wu, X. and Li, C. (2009) The Arabidopsis homologs of CCR4-associated factor 1 show mRNA deadenylation activity and play a role in plant defence responses. *Cell Res.* **19**, 307–316.

Liu, L. and Chen, X. (2016) RNA quality control as a key to suppressing RNA silencing of endogenous genes in plants. *Mol. Plant.* **9**, 826–836.

Liu, Y., Schiff, M. and Dinesh-Kumar, S.P. (2002) Virus-induced gene silencing in tomato. *Plant J.* **31**, 777–786.

Liu, S.-W., Wyatt, L.S., Orandle, M.S., Minai, M. and Moss, B. (2014) The D10 decapping enzyme of vaccinia virus contributes to decay of cellular and viral mRNAs and to virulence in mice. *J. Virol.* **88**, 202–211.

Lloyd, R.E. (2012) How do viruses interact with stress-associated RNA granules? *PLoS Pathog.* **8**, e1002741.

Lloyd, R.E. (2014) Regulation of stress granules and P-bodies During RNA virus infection. *Wiley Interdiscip RNA* **4**, 317–331.

Luo, Z. and Chen, Z. (2007) Improperly terminated, unpolyadenylated mRNA of sense transgenes is targeted by RDR6-mediated RNA silencing in Arabidopsis. *Plant Cell*, **19**, 943–958.

Maldonado-Bonilla, L.D. (2014) Composition and function of P bodies in Arabidopsis thaliana. *Front. Plant Sci.* **5**, 201.

Martinez de Alba, A.E., Moreno, A.B., Gabriel, M. et al. (2015) In plants, decapping prevents RDR6-dependent production of small interfering RNAs from endogenous mRNAs. *Nucleic Acids Res.* **43**, 2902–2913.

Meng, Y., Shao, C., Wang, H. and Chen, M. (2011) The regulatory activities of plant microRNAs: a more dynamic perspective. *Plant Physiol.* **157**, 1583–1595.

Moon, S.L. and Wilusz, J. (2013) Cytoplasmic viruses: rage against the (cellular RNA decay) machine. *PLoS Pathog.* **9**, e1003762.

Moon, S.L., Barnhart, M.D. and Wilusz, J. (2012) Inhibition and avoidance of mRNA degradation by RNA viruses. *Curr. Opin. Microbiol.* **15**, 500–505.

Moreno, A.B., Martinez de Alba, A.E., Bardou, F., Crespi, M.D., Vaucheret, H., Maizel, A. and Mallory, A.C. (2013) Cytoplasmic and nuclear quality control and turnover of single-stranded RNA modulate post-transcriptional gene silencing in plants. *Nucleic Acids Res.* **41**, 4699–4708.

Mourrain, P., Béclin, C., Elmayan, T. et al. (2000) Arabidopsis SGS2 and SGS3 genes are required for posttranscriptional gene silencing and natural virus resistance. *Cell*, **101**, 533–542.

Narayanan, K. and Makino, S. (2014) Interplay between viruses and host mRNA degradation. *Biochim. Biophys. Acta* **1829**, 732–741.

Parrish, S., Resch, W. and Moss, B. (2007) Vaccinia virus D10 protein has mRNA decapping activity, providing a mechanism for control of host and viral gene expression. *Proc Nat. Ac. Sci.* **104**(7), 2139–2144.

Peragine, A., Yoshikawa, M., Wu, G., Albrecht, H.L. and Poethig, R.S. (2004) SGS3 and SGS2/SDE1/RDR6 are required for juvenile development and the production of trans-acting siRNAs in Arabidopsis. *Genes Dev.* **18**, 2368–2379.

Pfaffl, M.W. (2001) A new mathematical model for relative quantification in real-time RT-PCR. *Nucleic Acids Res.* **29**, e45. Available at: http://www.pubmedcentral.nih.gov/articlerender.fcgi?artid=55695&tool=pmcentrez&rendertype=abstract.

Potuschak, T., Vansiri, A., Binder, B.M., Lechner, E., Vierstra, R.D. and Genschik, P. (2006) The exoribonuclease XRN4 is a component of the ethylene response pathway in Arabidopsis. *Plant Cell*, **18**, 3047–3057.

Qu, F. and Morris, T.J. (2005) Suppressors of RNA silencing encoded by plant viruses and their role in viral infections. *FEBS Lett.* **579**, 5958–5964.

Qu, F., Ren, T. and Morris, T.J. (2003) The coat protein of turnip crinkle virus suppresses posttranscriptional gene silencing at an early initiation step the coat protein of turnip crinkle virus suppresses posttranscriptional gene silencing at an early initiation step. *Society*, **77**, 511–522.

Rodriguez, M., Conti, G., Zavallo, D., Manacorda, C. and Asurmendi, S. (2014) TMV-Cg coat protein stabilizes DELLA proteins and in turn negatively modulates salicylic acid-mediated defense pathway during. *BMC Plant Biol.* **14**, 210.

Roth, B.M., Pruss, G.J. and Vance, V.B. (2004) Plant viral suppressors of RNA silencing. *Virus Res.* **102**, 97–108.

Sarowar, S., Oh, H.W., Cho, H.S., Baek, K.-H., Seong, E.S., Joung, Y.H., Choi, G.J., Lee, S. and Choi, D. (2007) Capsicum annuum CCR4-associated factor CaCAF1 is necessary for plant development and defence response. *Plant J.* **51**, 792–802.

Schmid, M. and Jensen, T.H. (2008) The exosome : a multipurpose RNA-decay machine. *Trends Biochem. Sci.* **33**(10), 501–510.

Schoenberg, D.R. and Maquat, L.E. (2012) Regulation of cytoplasmic mRNA decay. *Nat. Rev. Genet.* **13**, 246–259.

Schwach, F., Vaistij, F.E., Jones, L. and Baulcombe, D.C. (2005) An RNA-dependent RNA Polymerase prevents meristem invasion by potato virus X and is required for the activity but not the production of a systemic silencing signal. *Plant Physiol.* **138**, 1842–1852.

Shamandi, N., Zytnicki, M., Charbonnel, C., Elvira-Matelot, E., Bochnakian, A., Comella, P., Mallory, A.C., Lepère, G., Sáez-Vásquez, J. and Vaucheret, H. (2015) Plants encode a general siRNA suppressor that is induced and suppressed by viruses. *PLoS Biol.* **13**, 1–28.

Shin, J.-H., Wang, H.-L.V., Lee, J., Dinwiddie, B.L., Belostotsky, D.A. and Chekanova, J.A. (2013) The role of the arabidopsis exosome in siRNA–independent silencing of heterochromatic loci A. Cheung, ed. *PLoS Genet.* **9**, e1003411.

Siddiqui, S.A., Sarmiento, C., Truve, E., Lehto, H. and Lehto, K. (2008) Phenotypes and functional effects caused by various viral RNA silencing suppressors in transgenic *N. benthamiana* and *N. tabacum. Mol. Plant Microbe Interact.* **21**, 178–187.

Thran, M., Link, K. and Sonnewald, U. (2012) The Arabidopsis DCP2 gene is required for proper mRNA turnover and prevents transgene silencing in Arabidopsis. *Plant J.* **72**(3), 368–377.

Va, A., Group, P.V., Havelda, Z., Várallyay, E., Válóczi, A. and Burgyán, J. (2008) Plant virus infection-induced persistent host gene downregulation in systemically infected leaves. *Plant J.* **55**, 278–288.

Vanacova, S. and Stefl, R. (2007) The exosome and RNA quality control in the nucleus. *EMBO Rep.* **8**, 651–657.

Vazquez, F., Rajagopalan, R., Lepers, C., Gasciolli, V., Mallory, A.C., Hilbert, J., Bartel, D.P. and Cre, P. (2004) Endogenous trans -Acting siRNAs regulate the accumulation of arabidopsis mRNAs. *Mol. Cell* **16**, 69–79.

White, J.P. and Lloyd, R.E. (2012) Regulation of stress granules in virus systems. *Trends Microbiol.* **20**(4), 175–183.

Whitham, S.A., Quan, S., Chang, H., Cooper, B., Estes, B., Zhu, T., Wang, X. and Hou, Y. (2003) Diverse RNA viruses elicit the expression of common sets of genes in susceptible Arabidopsis thaliana plants. *Plant J.* **33**, 271–283.

Whitham, S.A., Yang, C. and Goodin, M.M. (2006) Global impact: elucidating plant responses to viral infection. *Mol. Plant Microbe Interact.* **19**, 1207–1215.

Wieczorek, P. and Obrępalska-Stęplowska, A. (2014) Suppress to survive—implication of plant viruses in PTGS. *Plant Mol. Biol. Report.* **33**, 335–346.

Xu, J. and Chua, N.-H. (2011) Processing bodies and plant development. *Curr. Opin. Plant Biol.* **14**, 88–93.

Ye, J., Yang, J., Sun, Y., Zhao, P., Gao, S., Jung, C., Qu, J., Fang, R. and Chua, N.H. (2015) Geminivirus activates asymmetric leaves 2 to accelerate cytoplasmic DCP2-mediated mRNA turnover and weakens RNA silencing in arabidopsis. *PLoS Pathog.* **11**, 1–21.

Zavallo, D., Debat, H.J., Conti, G., Manacorda, C.A., Rodriguez, M.C. and Asurmendi, S. (2015) Differential mRNA accumulation upon early Arabidopsis thaliana infection with ORMV and TMV-Cg is associated with distinct endogenous small RNAs level. *PLoS ONE*, **10**, 1–24.

Zhang, X., Zhu, Y., Liu, X. et al. (2015) Suppression of endogenous gene silencing by bidirectional cytoplasmic RNA decay in Arabidopsis. *Plant Biol.* **348**, 120–124.

Zhang, X., Zhu, Y., Wu, H. and Guo, H. (2016) Post-transcriptional gene silencing in plants: a double-edged sword. *Sci. China. Life Sci.* **59**(3), 271–276.